RESEARCH ARTICLE

MR Imaging Features of Basal Cell Adenoma of the Parotid Gland: Differentiation from Pleomorphic Adenoma and Warthin Tumor

Ming-Wei Xie[1], Zi-Liang Cheng[1], Hai-Yan Wang[2], Guang-Zi Shi[1], Hui-Jun Hu[1], Zhi-Long Yi[1], Wan-Shao Lin[1] and Zhuo Wu[1]*

[1]Department of Radiology, Sun Yat-Sen Memorial Hospital, Sun Yat-Sen University, Guangdong, 510120, China

[2]Department of Radiology, Jiangsu Cancer Hospital, Nanjing, Jiangsu, 510120, China

*Corresponding author: *Zhuo Wu, Department of Radiology, Sun Yat-Sen University, Sun Yat-Sen Memorial Hospital, No. 107 Yanjiang Road West, Guangzhou 510120, China, Tel: +862-081-332-702, Fax: +862-081-332-702, E-mail: vojoan@hotmail.com*

Abstract

Purpose: To identify the distinctive MR imaging features of basal cell adenoma (BCA) from pleomorphic adenoma (PA) and Warthin tumor (WT) in the parotid gland.

Methods: MR imaging features of 105 consecutive patients with histologically confirmed BCAs (n = 9), PAs (n = 59) or WTs (n = 37) were assessed.

Results: Compared with PAs, more BCAs were regular shape (P = 0.046) and had a solid portion with low T2 SI (P = 0.001). Compared with WTs, more BCAs had a solid portion showing marked enhancement on fat-suppressed T1 weighted images (P < 0.001).

Conclusion: T2 and enhanced T1 SI are useful for the differentiation between BCA and PA or WT.

Keywords

Adenoma, Parotid neoplasms, Magnetic resonance imaging, Retrospective studies, Comparative study

Introduction

Basal cell Adenoma (BCA) is an uncommon, benign epithelial tumor of the parotid gland, accounting for approximately 1%-3% of all parotid gland benign tumors [1,2]. Pleomorphic adenoma (PA) and Warthin tumor (WT) are the other two most popular benign parotid gland tumors. BCA is the third most common benign parotid tumors, following WT and PA. The incidence of BCA is far less than parotid PA and WT, but the main clinical presentations of BCA such as slow-growing, asymptomatic painless mass, and well-defined cystic or solid masses are extremely similar to PA or WT. The appropriate treatment is critical for these tumors. For example, enucleation for WT leads to approximately 2% recurrence rate, while that for PA is reported to reach 85%, and recurrence of BCA has been reported to be rare [3-5]. The treatment of BCAs is surgical excision by means of a superficial or total parotidectomy in cases in which parotid affectation exists [6]. Usually, superficial parotidectomy is performed for tumors in the superficial lobe, while subtotal parotidectomy is done for tumors in the deep lobe.

Fine needle aspiration cytology (FNAC) is a preoperatively diagnostic choice. Whereas FNAC could lead to a risk of possible spread of tumor cells, which can elevate the likelihood of local recurrence [7]. To date, CT or MR imaging has become a routine preoperative workup for the diagnosis of parotid gland tumors.

CT imaging features of BCA, PA and WT had been well described. For example, BCA is featured as intratumor cystic areas, linear bands or stellate-shaped non-enhanced areas [8]. PA manifests as multinodular enhancement on the early-phase and increased enhancement on the delayed phase on dynamic contrast-enhanced CT [9,10]. WT shows a pattern of strong enhancement on the early phase but decreased enhancement on the delayed phase [9,11]. Two types of enhancement patterns BCA were reported [12]. So far, MR imaging has been increasingly used for the diagnosis of parotid tumors. Recently, several new MR tech-

Ming-Wei et al. Int J Radiol Imaging Technol 2018, 4:033

• Page 1 of 7 •

niques have been reported to be useful in diagnosis of parotid tumors, such as arterial spin labelling-based perfusion MR imaging and diffusion-weighted imaging [13,14]. Because of the technique limitation and accompanied additional expenses, conventional MR imaging remains the mainstay of preoperative diagnostic means for parotid tumors. Previously, the clinicopathological features of BCA versus PA and WT have been described [2]. However, unlike PA and WT, MR imaging features of BCA have not been well described.

In this study, we retrospectively analyzed the MR imaging findings in large series including 9 patients with BCA, 59 patients with PA and 37 patients with WT. The purpose of this study is to identify characteristic MR imaging features of BCAs, which can be helpful for the differentiation between BCAs and PAs or WTs.

Materials and Methods

Patients

Between January 2010 and March 2016, 105 patients with pathologically confirmed parotid benign tumors including BCA (n = 9), PA (n = 59) and WT (n = 37) in our hospital were enrolled. All patients underwent MR imaging before surgery. The study was approved by the institutional review board of our institution, and patient informed consent was waived for this type of review. There were 68 men and 37 women, aged from 14 years to 87 years with a mean of 49 years. All patients were treated with surgical resection. The medical records of all patients are well maintained.

MR Imaging

MR imaging was performed in 43 patients by using a 1.5-T MR scanner (Gyroscan Intera; Philips Medical Systems, Best, Netherlands) and in 62 patients by using a 3.0-T MR scanner (Achieva; Philips Medical Systems, Netherlands) with a head and neck synergy coil to allow for coverage from the skull base to the thoracic inlet. MR protocol consisted of plain scan including axial Fast Spin Echo (FSE) T1 and T2 weighted imaging and contrast-enhanced imaging. Axial T2 weighted imaging was acquired by using parameters as follows: TR/TE = 700/2.29 ms; matrix = 288 × 194, FOV = 230 × 230 × 143 mm, section thickness/gap = 4/1 mm. Axial T1 weighted imaging was acquired by using TR/TE = 476/20 ms; matrix = 288 × 194, FOV = 220 × 230 × 154 mm, section thickness/gap = 4/1 mm. After intravenous injection of gadopentetate dimeglumine (Magnevist, Schering, Berlin, Germany) at a dosage of 0.2 mL/kg body weight, fat-suppressed axial and coronal FSE T1 weighted imaging without fat-suppression were obtained with TR/TE: 512/20 ms, 550/18 ms; matrix: 276 × 220-200 × 166; FOV, 220 × 220 × 154 mm - 220 × 54 × 216 mm; section thickness/gap, 4/1 mm.

Imaging analysis

All MR images were reviewed on a picture archiving and communication systems (Centricity RIS CE 3.0; GE Healthcare, Milwaukee, WI, USA) by two experienced radiologists in consensus and in a blinded manner (Z.W, with 15 years of experience with diagnostic imaging, and M.W.X, with 8 years of experience with diagnostic imaging). MR imaging features including the number of tumors (solitary or multifocal), location, size, shape, capsule, signal intensity, intratumor cystic area and contrast enhancement pattern were determined. Tumor location was divided into superficial and deep parotid lobes on the right or left sides. Tumor size was measured in maximal dimension on the transverse plane. The shape of the lesion was classified as regular (round/ovoid) or lobulated. The signal intensity (SI) was assessed only for the solid portion of tumors. Tumor SIs were classified as hyperintense, hypointense and mixed hyper- and hypo-intense on T2 weighted images, and as hypointense and mixed hyper- and hypo-intense on T1 weighted images compared with the surrounding uninvolved parotid gland. Tumor enhancement was assessed on the fat-suppressed contrast-enhanced T1 weighted images. The degrees of enhancement were graded as mild (less or equal to the surrounding parotid tissues) and marked (higher than the parotid gland). The presence of unenhanced cystic area was recorded, and their patterns were categorized as round/ovoid or irregular, and the irregular unenhanced area represents a branched or strip shape. The presence of capsule was assessed.

Statistical analysis

Data was presented as a mean ± standard deviation and n (%). MR imaging features of the number of tumors (solitary or multifocal), location (left/right side or superficial/deep lobe), shape, capsule, signal intensity, intratumor cystic area and contrast enhancement were compared between BCA and PA/WT. The categorical variables were analyzed by using continuity corrected Chi-square test or Fisher's exact test. The size and patient age were compared by Mann-Whitney U test. All statistical tests were performed by using software (SPSS, version 17.0, Chicago, IL, USA). P-values < 0.05 were considered to indicate statistical significance.

Results

Characteristics of patients

The mean age of patients with BCAs was significantly greater than that in PAs (mean age ± SD 59.6 ± 8.7 versus 39.8 ± 14.5 years, P < 0.001). No significant difference was found in sex distribution between BCAs and PAs or WTs (P < 0.474) (Table 1). Three PA patients had two tumors. Ten WT patients had multiple tumors, including 2 in 5 patients, 4 in 4 patients and 5 in 1 patient. The number of lesions of BCAs, PAs and WTs were 9, 62 and 58, respectively (Table 1).

MR imaging features

The MR imaging features in BCAs, PAs and WTs are

Table 1: Characteristics of patients with BCA, PA and WT.

	BCA (n = 9)	PA (n = 59)	P-values (PA vs. BCA)	WT (n = 37)	P-values (WT vs. BCA)
Age	59.6 ± 8.7	39.8 ± 14.5	< 0.001#	61.5 ± 16.5	0.627#
Number			1.000‡		= 0.189†
Solitary	9 (100)	56 (94.92)		27 (72.97)	
Multifocal	0 (0)	3 (5.08)		10 (27.03)	
Sex			0.474†		0.143†
Female	3 (33.33)	31 (52.54)		3 (8.11)	
Male	6 (66.67)	28 (47.46)		34 (91.89)	

Data are expressed as mean ± standard deviation for continuous variables or numbers of patients with percentages in parentheses. †P value by the continuity corrected Chi-square test; ‡P value by Fisher's exact test; #P value by Mann-Whitney U test. BCA: Basal cell adenoma; PA: Pleomorphic adenoma; WT: Warthin tumor.

Table 2: MR Imaging findings of BCAs, PAs and WTs.

	BCA (n = 9)	PA (n = 62)	P-values (PA vs. BCA)	WT (n = 58)	P-values (WT vs. BCA)
Right/left side			0.827†		0.703†
Right side	6 (66.67)	35 (56.45)		31 (53.45)	
Left side	3 (33.33)	27 (43.55)		27 (46.55)	
Location			0.346‡		0.430‡
Superficial lobe	6 (66.67)	42 (67.74)		37 (63.79)	
Deep lobe	0 (0)	9 (14.52)		9 (15.52)	
Both lobes	3 (33.33)	11 (17.74)		12 (20.69)	
Size					
Maximum (mm)	22.7 ± 9.8	24.8 ± 10.0	0.523#	23.5 ± 13.4	0.769#
Shape			0.046†		0.142†
Round/ovoid	9 (100)	37 (59.68)		41 (70.69)	
Lobulated	0 (0)	25 (40.32)		17 (29.31)	
Capsule			1.000‡		1.000‡
Presence	9 (100.00)	60 (96.77)		54 (93.10)	
Absence	0 (0)	2 (3.23)		4 (6.90)	
T2 SI			0.001‡		0.13‡
Hyperintensity	0 (0)	11 (11.74)		0 (0)	
Mixed hyper- and hypointensity	2 (22.22)	43 (69.36)		3 (5.17)	
Hypointensity	7 (77.78)	8 (12.90)		55 (94.83)	
T1 SI			0.426‡		0.252‡
Hypointensity	8 (88.89)	59 (95.16)		57 (98.28)	
Mixed hypo- and hyperintensity	1 (11.11)	3 (4.84)		1 (1.72)	
Enhancement			0.124†		< 0.001†
Marked	9 (100)	43 (69.35)		3 (5.17)	
Mild	0 (0)	14 (30.65)		55 (94.83)	
Cystic area			0.052‡		0.056‡
Irregular	3 (33.33)	4 (6.45)		3 (5.17)	
Round/ovoid	3 (33.33)	24 (38.71)		26 (44.83)	
Absence (solid)	3 (33.33)	34 (54.84)		29 (50)	

Data are expressed as mean ± standard deviation for continuous variables or numbers of lesions with percentages in parentheses. †P value by the continuity corrected Chi-square test; ‡P value by Fisher exact test; #P value by Mann-Whitney U test; BCA: Basal cell adenoma; PA: Pleomorphic adenoma; WT: Warthin tumor; SI: Signal intensity; T2: T2-weighted imaging; T1: Fat-suppressed T1 weighted imaging.

summarized in Table 2. BCAs, PAs and WTs tended to locate in the right side of the parotid gland. Six of 9 BCAs (66.67%), 35 of 62 PAs (56.45%) and 31 of 58 WTs (53.45%) were located in the right parotid gland (Figure 1, Figure 2, Figure 3, Figure 4, Figure 5, Figure 6 and Figure 7), while no significant difference was found (P = 0.703-0.827). All BCAs have a round or ovoid shape, whereas 59.68% of PAs (37/62) and 70.69% of WTs (41/58) have a lobulated shape. There was a significant difference between BCAs and PAs (P = 0.046), but there

was no significant difference with respect to the location, tumor size, and capsule among three types of tumors (P = 0.346-1.000) (Table 2).

The solid portion of tumors in 7 of 9 BCAs (77.78%) and 8 of 62 PAs (12.90%) were hypointense on T2 weighted imaging. Two of 9 BCAs (22.22%) and 43 of 62 PAs (69.36%) showed mixed hyper- and hypointense, and 11 of 62 PAs (11.74%) showed hyperintense on T2 weighted imaging (Figure 4 and Figure 5). No lesion has
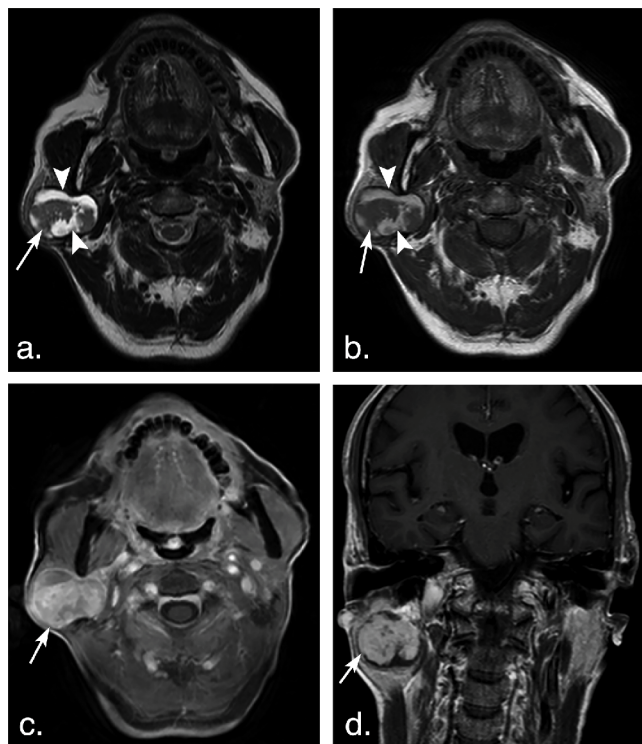
Figure 1: A 75-year-old man with basal cell adenoma in both superficial and deep lobes in the right parotid gland. Axial T2 weighted image (a) and axial T1 weighted image (b) show a well-defined, encapsulated, heterogeneous, lobulated tumor with irregular cystic area (arrowheads) and solid nodule (arrows). The solid portion of the tumor shows hypoinentse signal on T2 weighted and T1 weighted images and marked enhancement (arrow) compared with the surrounding parotid gland on axial contrast-enhanced fat-suppressed T1 weighted image (c) but mild enhancement (arrow) on coronal non-fat suppressed T1 weighted image (d) (arrows).
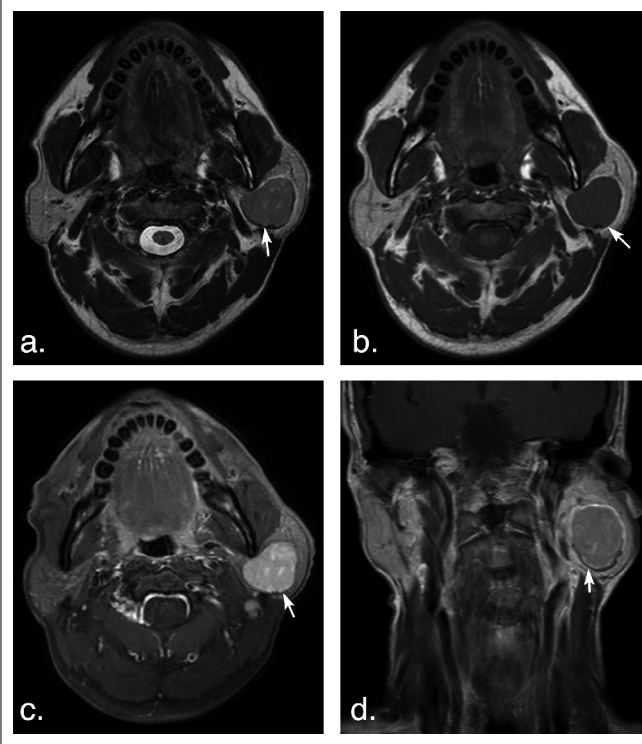

Figure 2: A 53-year-old man with basal cell adenoma in the deep lobe of the left parotid gland. Axial T2 weighted image (a) and T1 weighted image (b) shows a well-defined, ovoid solid-looking tumor (arrows). The tumor shows slight hypointense signal on T2 weighted image and T1 weighted image, marked enhancement (arrow) on axial contrast-enhanced fat-suppressed T1 weighted image (c) but mild enhancement (arrow) on coronal non-fat suppressed T1 weighted image (d).

hyperintense signal in BCAs and WTs on T2 weighted imaging (Figure 1, Figure 2, Figure 3, Figure 4, Figure 5 and Figure 6). There was significant difference between BCAs and PAs (P < 0.001).

Enhancement of tumor solid portion on the delayed phase of fat-suppressed contrast-enhanced T1 weighted imaging was significantly different between BCAs and WTs (P < 0.001). All lesions of BCAs and 43 of 62 (69.35%) PAs showed marked enhancement, while only 3 in 58 WTs were markedly enhanced (Figure 1, Figure 2, Figure 3, Figure 4, Figure 5 and Figure 6). No significant difference was found between BCAs and PAs (P = 0.0124).

Three of 9 BCAs (33.33%), 34 of 62 PAs (54.84%) and 29 of 58 WTs (50%) were solid-looking tumors. Three of 9 BCAs (33.33%), 4 of 62 PAs (6.45%) and 3 of 58 WTs (5.17%) had an irregular nonenhanced cystic area within the tumor. Three of 9 BCAs (33.33%), 24 of 62 PAs (38.71%) and 26 of 58 WTs (44.83%) had an ovoid nonenhanced cystic area within the tumors (Figure 7). There was no significant difference between BCA and PA (P = 0.052), and between BCA and WT (P = 0.056).

Discussion

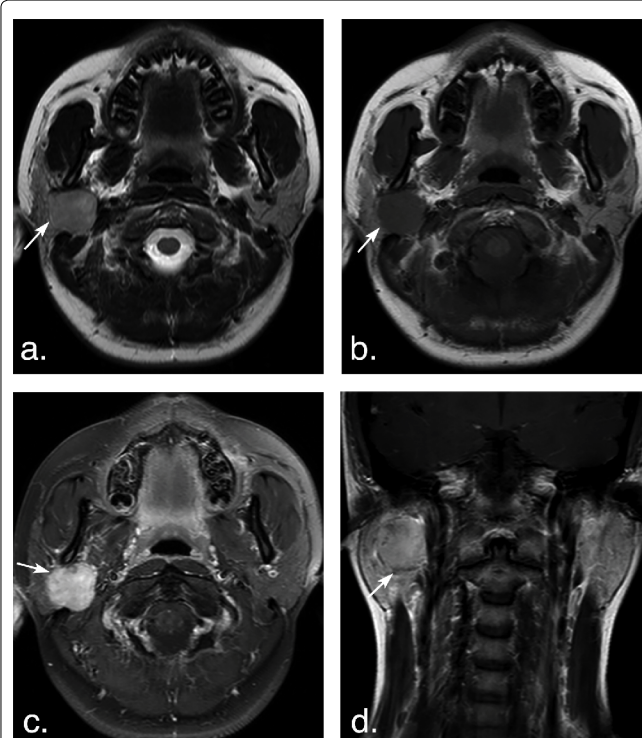BCAs are the rare, benign epithelial tumor and lacks

Figure 3: A 14-year-old woman with pleomorphic adenoma in the deep lobe of the right parotid gland. T2 weighted image (a) and T1 weighted image (b) show a well-defined, lobulated tumor (arrows). The tumor shows hyperintense signal on T2 weighted image and hypointense signal on T1 weighted image, marked enhancement (arrow) on axial contrast-enhanced fat-suppressed T1 weighted image (c) but mild enhancement (arrow) on coronal non-fat suppressed T1 weighted image (d).
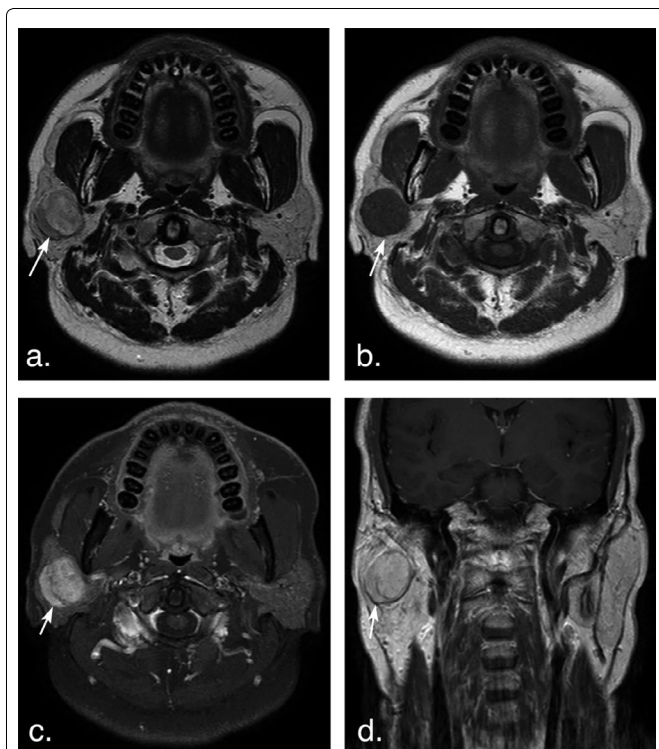
Ming-Wei et al. Int J Radiol Imaging Technol 2018, 4:033

• Page 4 of 7

Figure 4: A 51-year-old man with pleomorphic adenoma in the superficial lobe of the right parotid gland. T2 weighted image (a) and T1 weighted image (b) show a well-defined, heterogeneous tumor (arrows). The tumor shows hyperintense signal on T2 weighted image and hypointense signal on T1 weighted image, marked enhancement (arrow) on axial contrast-enhanced fat-suppressed T1 weighted image (c) but mild enhancement (arrow) on coronal non-fat suppressed T1 weighted image (d).

Figure 5: A 63-year-old man with Warthin tumors in the deep lobe of the left parotid gland. T2 weighted image (a) and T1 weighted image (b) show a well-defined, lobulated, heterogonous tumor. Lesion with irregular cystic area (arrowheads) and solid nodule (arrows). The solid portion of the tumor shows hypoinentse signal on T2 weighted and T1 weighted MR images, and mild enhancement (arrow) on axial contrast-enhanced fat-suppressed T1 weighted image (c) and coronal non-fat suppressed T1 weighted image (d) (arrows).

the mesenchyme-like component that pleomorphic adenomas possess [15,16]. Their CT, MR or ultrasound imaging features are characterized as a round, well-defined, obviously enhanced solid mass with or without a cystic portion [12,17,18]. In this study, all BCAs had an ovoid shape, which is significantly different from PAs, as most of PAs (59.68%) showed lobulated contour. This might be caused by the different growth rates of different cell types within the tumor of PA. Moreover, PAs have abundant myxoid areas histologically and incomplete encapsulation, which can lead to a lobulated contour [19,20].

The hypointense signal of solid portion on T2 weighted imaging was observed in all cases of BCAs in our study. This finding is in consistence with that by Okahara, et al. [17]. Benign PAs usually show bright signal intensity on T2 weighted images because of an area containing abundant fibromyxoid stroma [19,21]. In our series, more than 80% of PAs had the area of high signal intensity on T2 weighted images. The lower signal intensity than surrounding normal parotid gland on T2 weighted images might be a useful feature for differentiating BCA from PA. This low signal intensity on T2 weighted images probably corresponds to the high cellularity. WT shows similar hypointense signal on T2 weighted images as BCA. Such hypointense signal was reported to be caused by the cellular components with
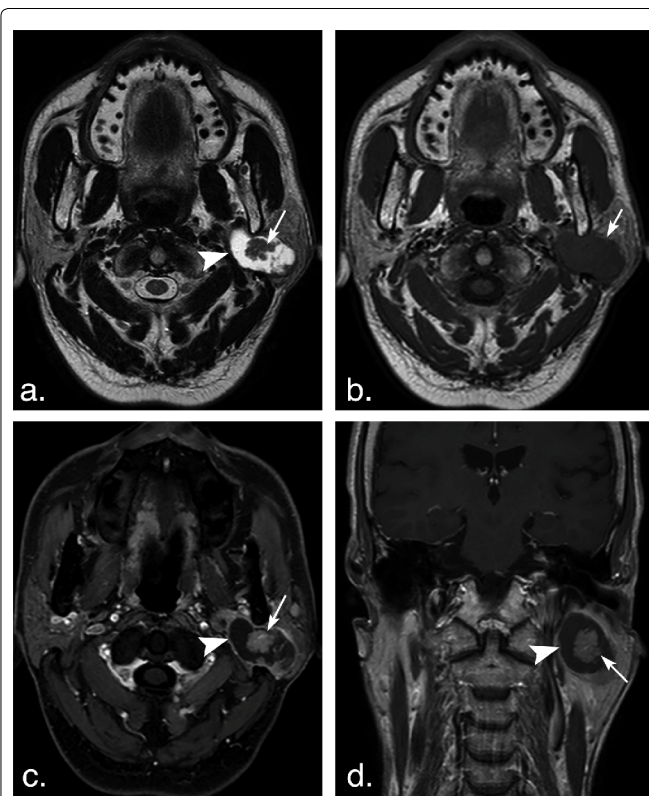
accumulated microscopic cysts containing proteinous fluid with foamy cells, red cells, and neutrophils [11].

The marked enhancement of solid portion on the fat-suppressed contrast-enhanced T1 weighted images was found in all cases of BCAs in our study. However, in the study by Okahara, et al. such characteristic feature of marked enhancement has not been described [17]. Unlike non-fat-suppressed contrast-enhanced T1 weighted imaging applied in most cases (7 of 8 patients) in their study [17], we used fat-suppressed T1-weighted images as regards fat tissue is a substantial component of the parenchyma of the parotid gland [22]. Such marked enhancement on the fat-suppressed T1-weighted images is useful for the distinction BCA from WT, which is characterized by mild enhancement on the venous phase due to early enhancement and subsequent washout pattern on dynamic study [11]. Lee, et al. reported that on CT imaging BCAs with large cystic areas showed gradual and additional enhancement on the delayed phase, and mostly solid-looking BCAs showed marked contrast enhancement on the early phase and a subsequent decrease on the delayed phase [11]. In our study, we found both types of BCAs showed obvious enhancement on the contrast-enhanced T1 weighted imaging. This difference might be related to the distinc-

Table 3: Signal intensity and enhancement of BCAs, PAs and WTs.

	BCA	PA	WT
T2 SI	Mainly hypointensity	Mainly mixed hyper- and hypointensity	Mainly hypointensity
T1 SI	Mainly hypointensity	Mainly hypointensity	Mainly hypointensity
Enhancement	Marked	Mainly marked	Mainly mild

PA: Pleomorphic adenoma; WT: Warthin tumor; SI: Signal intensity; T2: T2-weighted imaging; T1: Fat-suppressed T1-weighted imaging.
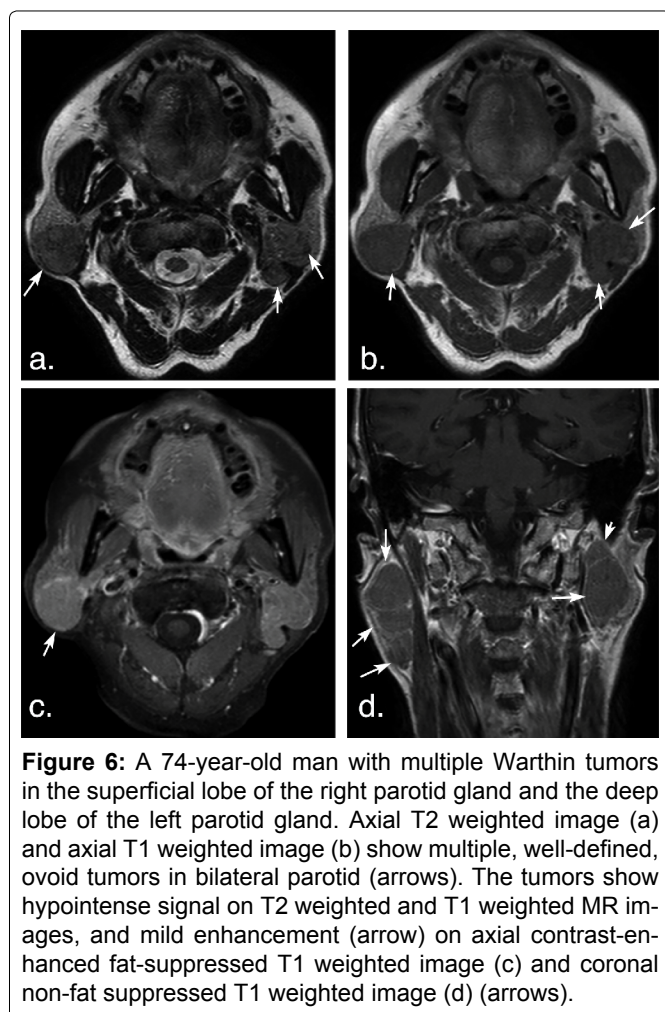

Figure 6: A 74-year-old man with multiple Warthin tumors in the superficial lobe of the right parotid gland and the deep lobe of the left parotid gland. Axial T2 weighted image (a) and axial T1 weighted image (b) show multiple, well-defined, ovoid tumors in bilateral parotid (arrows). The tumors show hypointense signal on T2 weighted and T1 weighted MR images, and mild enhancement (arrow) on axial contrast-enhanced fat-suppressed T1 weighted image (c) and coronal non-fat suppressed T1 weighted image (d) (arrows).

Figure 7: Different shape of the cystic areas in the parotid gland tumors. (a) T2 weighted image shows a large ovoid cystic hyperintense cystic area (arrow) in a basal cell adenoma of a 57-year-old man. (b) T2 weighted image shows several ovoid cystic hyperintense cystic areas (arrows) in Warthin tumors of a 52-year-old man. (c) T2 weighted image shows a small round cystic hyperintense cystic area (arrow) in the heterogeneous pleomorphic adenoma of a 39-year-old female with on. (d) T2 weighted image shows a small ovoid cystic hyperintense cystic area (arrow) in a Warthin tumor of an 84-year-old man.

tive kinetics and imaging properties of different contrast media used in CT and MR imaging. PAs show marked enhancement on the fat-suppressed contrast-enhanced T1 weighted imaging in our study, which is consistent with the previously reported gradual increased enhancement pattern of PA [9,23] (Table 3).

In our study, the frequency of solid-looking BCAs (33.33%) was lower than that of PAs (54.84%) and WTs (50%). Most of BCAs had a cystic area. The cystic space of BCAs is lined with attenuated thin epithelium and contained some proteinaceous material or hemorrhage [24]. Interestingly, we found that more BCAs had an irregular cystic area than PAs and WTs. Notably, this finding has not been previously recorded.

In conclusion, BCAs of the parotid gland are frequently manifested as a round/ovoid mass with or without cystic areas. The frequency of cystic BCAs is higher than solid-looking BCAs. The solid portion of BCAs commonly exhibit low signal intensity on T2 weighted imaging and
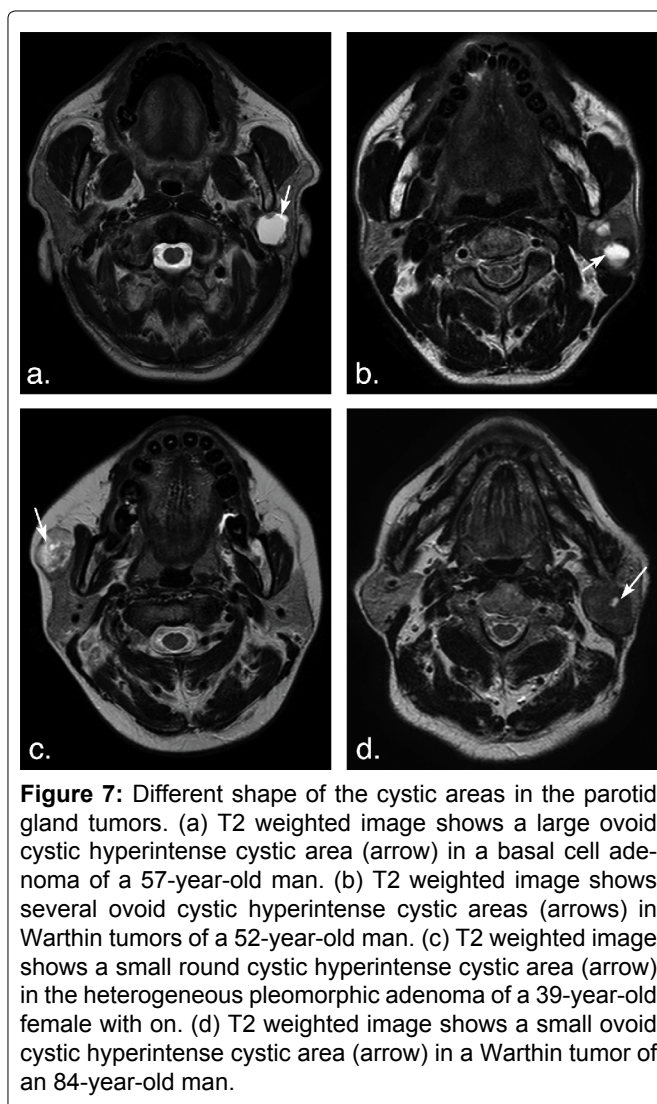
marked enhancement on the fat-suppressed T1-weighted imaging. PA is more likely to exhibit mixed hyper- and hypointense on T2 weighted imaging, lobulated shape and associated with younger age compared with BCA. WT is featured by mild enhancement on the fat-suppressed T1-weighted imaging. A regular tumor with a solid portion showing T2 hypointense signal but marked enhancement will highly favor a diagnosis of BCA in the parotid.

References

1. Nagao K, Matsuzaki O, Saiga H, Sugano I, Shigematsu H, et al. (1982) Histopathologic studies of basal cell adenoma of the parotid gland. Cancer 50: 736-745.

2. Kawata R, Yoshimura K, Lee K, Araki M, Takenaka H, et al. (2010) Basal cell adenoma of the parotid gland: a clinico-pathological study of nine cases-basal cell adenoma versus pleomorphic adenoma and Warthin's tumor. Eur Arch Otorhinolaryngol 267: 779-783.

Ming-Wei et al. Int J Radiol Imaging Technol 2018, 4:033

• Page 6 of 7 •

3. Swoboda H, Franz P (1994) Salivary gland tumors. Clinical aspects and therapy. Radiologe 34: 232-238.

4. Heller KS, Attie JN (1988) Treatment of Warthin's tumor by enucleation. Am J Surg 156: 294-296.

5. Witt RL (2002) The significance of the margin in parotid surgery for pleomorphic adenoma. Laryngoscope 112: 2141-2154.

6. Kanaujia SK, Singh A, Nautiyal S, Ashutosh K (2015) Basal cell adenoma of parotid gland: Case report and review of literature. Indian J Otolaryngol Head Neck Surg 67: 430-433.

7. Das DK, Petkar MA, Al-Mane NM, Sheikh ZA, Mallik MK, et al. (2004) Role of fine needle aspiration cytology in the diagnosis of swellings in the salivary gland regions: A study of 712 cases. Med Princ Pract 13: 95-106.

8. Chawla AJ, Tan TY, Tan GJ (2006) Basal cell adenomas of the parotid gland: CT scan features. Eur J Radiol 58: 260-265.

9. Choi DS, Na DG, Byun HS, Ko YH, Kim CK, et al. (2000) Salivary gland tumors: Evaluation with two-phase helical CT. Radiology 214: 231-236.

10. Lev MH, Khanduja K, Morris PP, Curtin HD (1998) Parotid pleomorphic adenomas: Delayed CT enhancement. AJNR Am J Neuroradiol 19: 1835-1839.

11. Ikeda M, Motoori K, Hanazawa T, Nagai Y, Yamamoto S, et al. (2004) Warthin tumor of the parotid gland: Diagnostic value of MR imaging with histopathologic correlation. AJNR Am J Neuroradiol 25: 1256-1262.

12. Lee DK, Chung KW, Baek CH, Jeong HS, Ko YH, et al. (2005) Basal cell adenoma of the parotid gland: Characteristics of 2-phase helical computed tomography and magnetic resonance imaging. J Comput Assist Tomogr 29: 884-888.

13. Kato H, Kanematsu M, Watanabe H, Kajita K, Mizuta K, et al. (2015) Perfusion imaging of parotid gland tumours: Usefulness of arterial spin labeling for differentiating Warthin's tumours. Eur Radiol 25: 3247-3254.

14. Yerli H, Agildere AM, Aydin E, Geyik E, Haberal N, et al. (2007) Value of apparent diffusion coefficient calculation in the differential diagnosis of parotid gland tumors. Acta Radiol 48: 980-987.

15. Jang M, Park D, Lee SR, Hahm CK, Kim Y, et al. (2004) Basal cell adenoma in the parotid gland: CT and MR findings. AJNR Am J Neuroradiol 25: 631-635.

16. Koyuncu M, Seşen T, Akan H, Ismailoglu AA, Tanyeri Y, et al. (2003) Comparison of computed tomography and magnetic resonance imaging in the diagnosis of parotid tumors. Otolaryngol Head Neck Surg 129: 726-732.

17. Okahara M, Kiyosue H, Matsumoto S, Hori Y, Tanoue S, et al. (2006) Basal cell adenoma of the parotid gland: MR imaging findings with pathologic correlation. AJNR Am J Neuroradiol 27: 700-704.

18. Shi L, Wang YX, Yu C, Zhao F, Kuang PD, et al. (2012) CT and ultrasound features of basal cell adenoma of the parotid gland: A report of 22 cases with pathologic correlation. AJNR Am J Neuroradiol 33: 434-438.

19. Tsushima Y, Matsumoto M, Endo K, Aihara T, Nakajima T (1994) Characteristic bright signal of parotid pleomorphic adenomas on T2-weighted MR images with pathological correlation. Clin Radiol 49: 485-489.

20. Mărgăritescu C, Raica M, Simionescu C, Mogoantă L, Surpăţeanu M, et al. (2005) Tumoral stroma of salivary pleomorphic adenoma-histopathological, histochemical and immunohistochemical study. Rom J Morphol Embryol 46: 211-223.

21. Okahara M, Kiyosue H, Hori Y, Matsumoto A, Mori H, et al. (2003) Parotid tumors: MR imaging with pathological correlation. Eur Radiol 4: 25-33.

22. Sumi M, Takagi Y, Uetani M, Morikawa M, Hayashi K, et al. (2002) Diffusion-weighted echoplanar MR imaging of the salivary glands. AJR Am J Roentgenol 178: 959-965.

23. Takashima S, Noguchi Y, Okumura T, Aruga H, Kobayashi T (1993) Dynamic MR imaging in the head and neck. Radiology 189: 813-821.

24. Jeong AK, Lee HK, Kim SY, Cho KJ (2001) Basal cell adenoma in the parapharyngeal space: MR findings. Clin Imaging 25: 392-395.